Available online at www.sciencedirect.com
SCIENCE DIRECT®
Biochemical Pharmacology 68 (2004) 2207–2219
Biochemical Pharmacology
www.elsevier.com/locate/biochempharm

Effects of anandamide on the binding and signaling properties of M_1 muscarinic acetylcholine receptors

Alfred A. Lanzafame[1], Elizabeth Guida, Arthur Christopoulos*

Department of Pharmacology, University of Melbourne, Grattan Street, Parkville, Vic. 3010, Australia

Received 18 March 2004; accepted 6 August 2004

Abstract

This study investigated the effects of the endocannabinoid, anandamide, on M_1 muscarinic acetylcholine receptors (mAChRs) expressed in Chinese hamster ovary (CHO) cells. In the presence of anandamide, [^{3}H]*N*-methylscopolamine ([^{3}H]NMS) inhibition binding was characterized by Hill coefficients greater than 1 while saturation binding isotherms were characterized by a reduction in radioligand B_{max}. Anandamide did not affect the potency of classic agonists, antagonists or allosteric modulators to inhibit [^{3}H]NMS binding, indicating that the site of anandamide action did not involve receptor regions recognized by these compounds. Although the mode of binding of anandamide was reversible, the order of ligand addition was important; the inhibitory effect was greatest when anandamide was equilibrated with the receptor prior to radioligand addition, and weakest in the converse situation. Interestingly, the inhibitory potency of anandamide was reduced on pre-equilibration with non-transfected CHO cell membranes, prior to addition of M_1 mAChR-transfected membranes. In phosphoinositide (PI) hydrolysis assays, anandamide significantly reduced the maximal response to acetylcholine, but at higher concentrations than those needed to fully inhibit radioligand binding. Studies utilizing a range of agonists with varying intrinsic activities showed that the inhibitory effects of anandamide on agonist function were most pronounced with the lowest efficacy agonists. These findings suggest that the mechanism of action of anandamide at the M_1 mAChR involves perturbation of the receptor via the membrane in a manner that is sensitive to the conformation of the receptor (occupied versus vacant).

Keywords: Anandamide; Muscarinic acetylcholine receptor; Endocannabinoid; Radioligand binding; Phosphoinositide accumulation; Non-competitive interaction

It is well established that cholinergic and cannabinoid systems play important roles in the central nervous system. In particular, acetylcholine (ACh) and cannabinoid agonists are involved in the facilitation or disruption of learning and memory, respectively [1–5]. While the effects of ACh and cannabinoids are predominantly initiated by interaction with separate families of G protein-coupled receptors (GPCRs) [6–9], there is also a significant element of cross talk between the two receptor systems. For instance, cannabinoids have long been known to exert negative modulatory effects on the synthesis [10] and/or release of ACh [11], and more recent investigations have also demonstrated physiological antagonism between central cholinergic and cannabinoid mechanisms in their effects on memory processes [12,13].

The identification of an endogenous cannabinoid-signaling system, exemplified by agonists such as anandamide (Fig. 1) and 2-arachidonylglycerol, has led to studies of endocannabinoids that have revealed a potential for anandamide to exert direct modulatory actions on other receptor systems irrespective of, or in addition to, its ability to activate cannabinoid receptors. For example, neurobehavioral studies carried out in cannabinoid CB_1 GPCR knockout mice showed that, regardless of the lack of CB_1 receptors, anandamide still exerted cannabimimetic-like activity, even though the CB_1 GPCR was believed to be the only receptor for cannabinoids in the brain [14]. In vitro

Abbreviations: ACh, acetylcholine; BCh, butyrylcholine; CHO, Chinese hamster ovary; CNS, central nervous system; DMEM, Dulbeccos modified eagles medium; dpm, disintegrations per minute; GPCRs, G protein-coupled receptors; [^{3}H]GTPγS, guanosine 5′-*O*-(3-thiotriphosphate); 5-HT, 5-hydroxytryptamine; mAChR, muscarinic acetylcholine receptor; NMS, *N*-methylscoplamine; NT CHO, non-transfected CHO; Oxo-M, oxotremorine-M; PBZ, phenoxybenzamine; PI, phosphoinositide; QNB, quinuclidinyl benzilate; TMA, tetramethylammonium

* Corresponding author. Tel.: +61 3 8344 8417; fax: +61 3 8344 0241.
E-mail address: arthurc1@unimelb.edu.au (A. Christopoulos).
[1] Present address: Department of Pharmacology, Monash University, Clayton 3800, Australia.

0006-2952/$ – see front matter © 2004 Elsevier Inc. All rights reserved.
doi:10.1016/j.bcp.2004.08.005

Anandamide

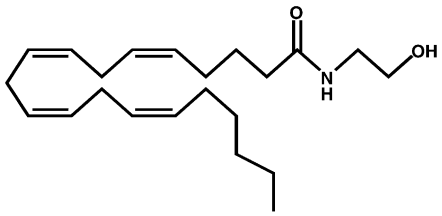

N-methylscopolamine

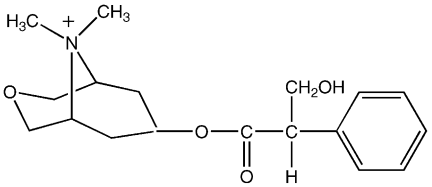

Butyrylcholine

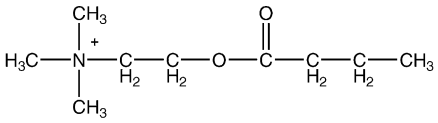

Acetylcholine

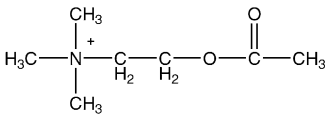

Choline

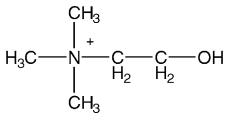

Tetramethylammonium

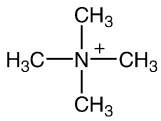

Fig. 1. Structures of ligands used in this study.

studies have also found that anandamide stimulated [^{3}H]GTPγ-S binding in brain membranes from CB_1 knockout mice that was insensitive to both CB_1 and CB_2 GPCR antagonism [14]. Further, evidence against CB_1 and CB_2 receptors being the sole targets for anandamide was obtained when the endocannabinoid was found to activate the capsaicin VR_1 vanilloid receptor [15–17].

Although the VR_1 receptor is an ion channel, anandamide has also been shown to inhibit ligand binding to central 5-HT GPCRs [18], suggesting that elevated local concentrations of the endocannabinoid, as found for example in schizophrenia [19] and ischaemia [20], can exert direct effects on certain receptors beyond those identified as the cognate receptors for this ligand. Given that cannabinoid receptors and muscarinic acetylcholine receptors (mAChRs) are also co-localized in some parts of the brain, it is possible that elevated anandamide levels may exert a "spill over" effect on mAChR binding and/or functional properties. Indeed, anandamide, and the structurally related arachidonic acid, have been shown to inhibit agonist as well as antagonist binding to mAChRs in human brain homogenates [21]. More recently, we have extended these findings by investigating the antagonistic effects of anandamide on M_1 and M_4 mAChRs expressed individually in CHO cells [22].

The aim of the present study was to determine what aspects of mAChR ligand pharmacology are sensitive to the effects of anandamide, and to further probe the possible mechanistic basis of the interaction between anandamide and the M_1 mAChR. This study provides evidence that the interaction of anandamide with the M_1 mAChR, involves a site distinct from the sites to which agonists, competitive antagonists and certain allosteric modulators bind, and is likely exerted through perturbation of the cell membrane in a mAChR occupancy-dependent manner.

1. Materials and methods

1.1. Materials

Drugs and chemicals were obtained from the following sources: [^{3}H]NMS from NEN Life Science Products, (Boston, MA, USA), [^{3}H]*myo*-inositol from Amersham Pharmacia Biotech (Buckinghamshire, UK), alcuronium chloride (generous gift from F. Hoffmann-La Roche Ltd., Basle, Switzerland), DMEM and geneticin were from Life Technologies GIBCO BRL (Grand Island, NY, USA), fetal bovine serum was from ThermoTrace, (Melbourne, VIC, Australia), and DOWEX AG1-X8 ion-exchange resin was obtained from Bio-Rad (Hercules, CA, USA). All other materials were from Sigma Chemical Company (St. Louis, MO, USA).

1.2. Cell culture

CHO-K1 cells, stably transfected with the human M_1 mAChR (M_1 CHO cells), were kindly provided by Dr. M. Brann, (University of Vermont Medical School, Burlington, VT). Cells were grown and maintained in DMEM containing 20 mM HEPES, 10% fetal bovine serum and 50 μg/ml geneticin for 4 days at 37 °C in a humidified incubator containing 5% CO_2:95% O_2, before harvesting by trypsinization followed by centrifugation (300 × *g*, 3 min) and resuspension of the pellet in DMEM.

1.3. Cell membrane preparations

M_1 CHO cells were grown, harvested and centrifuged as described above, with the final pellet resuspended in 5 ml of ice-cold Tris–HCl buffer (50 mM Tris, 3 mM $MgCl_2$ and 0.2 mM EGTA; pH 7.4 with HCl) and then homogenized using a Polytron homogenizer for three 10 s intervals at maximum setting with 30 s cooling periods employed between each burst. The cell homogenate was centrifuged

(1000 × *g*, 10 min, 25 °C), the pellet discarded and the supernatant was re-centrifuged at 30 000 × *g* for 30 min at 4 °C. The resulting pellet-containing cell membrane was resuspended in 5 ml of Tris–HCl buffer and protein content was determined using the method of Bradford [23]. The homogenate was then aliquoted into 1 ml amounts and stored frozen at −80 °C until required for radioligand binding assays.

1.4. Saturation binding assays

M_1 CHO cell membranes (5 μg/assay tube in a total volume of 1 ml) were incubated in HEPES buffer (110 mM NaCl, 5.4 mM KCl, 1.8 mM $CaCl_2$, 1 mM $MgSO_4$, 25 mM glucose, 50 mM HEPES, 58 mM sucrose; pH 7.4) with varying concentrations of [^{3}H]NMS (10 pM to 2 nM) in the absence and presence of different concentrations of anandamide (1, 5 or 10 μM) for 1 h at 37 °C. The reaction was then terminated by rapid filtration through Whatman GF/B filters using a Brandell cell harvester. Non-specific binding was determined using 10 μM atropine. Filters were washed three times with 4 ml aliquots of ice-cold saline and dried before radioactivity (dpm) was measured using liquid scintillation counting.

1.5. Inhibition binding assays

Experiments were performed on M_1 CHO cell membrane homogenates (5 μg/assay tube in a total volume of 1 ml) or intact cells (200 000 cells/assay tube in a total volume of 1 ml) for 1 or 4 h, as indicated in the Section 2. M_1 CHO cells were incubated with [^{3}H]NMS (0.2 nM) and various concentrations of anandamide (1 nM to 1 mM) for 1 h at 37 °C. In each experiment, a parallel curve was constructed with [^{3}H]NMS in combination with different dilutions of ethanol vehicle instead of anandamide concentrations. Other inhibition studies using membrane homogenates were conducted under similar conditions with [^{3}H]NMS (0.2 nM) and ACh (10 nM to 10 mM), Oxo-M (1 nM to 1 mM), xanomeline (0.1 nM to 0.1 mM), NMS (0.1 pM to 0.1 μM), QNB (0.1 pM to 0.1 μM), gallamine (1 nM to 1 mM), or alcuronium (1 nM to 10 mM) in the absence and presence of a fixed concentration of anandamide (3 μM) with an equilibration time of 1 h at 37 °C.

Additional inhibition binding studies were performed to determine whether the action of anandamide was via the cell membrane. Non-transfected (NT) CHO cell membranes (protein concentrations of 10, 15, 25, 50 or 100 μg/ assay tube in a total volume of 1 ml) were pre-incubated with anandamide (1 nM to 1 mM) and [^{3}H]NMS (0.2 nM) for 30 min before addition of M_1-expressing CHO cell membranes. Subsequently, a further 60 min equilibration period, at 37 °C, or a 3 h equilibration period, at 4 °C, was employed. In all cases, non-specific binding was determined using atropine (10 μM). All other details are as described above.

1.6. Dissociation kinetic assays

[^{3}H]NMS dissociation kinetic binding assays were performed using a reverse time protocol (0, 1, 3, 5, 10, 15, 20 and 30 min). In these experiments, M_1 CHO membranes (5 μg/assay tube in a total volume of 1 ml) were added to tubes containing [^{3}H]NMS (0.5 nM) in a time-staggered approach so that each replicate was allowed to equilibrate for 1 h at 37 °C. Once the receptors and radioligand had equilibrated, atropine (10 μM/assay tube in a total volume of 1 ml) in the absence and presence of anandamide (10 μM) was added at appropriate time intervals to prevent re-association of [^{3}H]NMS to the M_1 mAChR. In separate experiments, anandamide in the absence of atropine was added at the previously mentioned time points. Non-specific binding was determined using atropine (10 μM). All other details are as described above.

1.7. Anandamide washout and order-of-addition experiments

Intact M_1 CHO cells (200 000 cells/tube) were treated with anandamide (10 or 100 μM) for 1 h at 37 °C followed by extensive washout (4 ml × 10 ml HEPES buffer washes; 5 min/wash) before addition of a fixed concentration of [^{3}H]NMS (2 nM), and then the reaction was allowed to proceed for a further 2 h. A parallel study was also conducted examining the order of addition of anandamide and [^{3}H]NMS (2 nM). Anandamide was either preincubated with M_1 CHO cells for 30 min before addition of [^{3}H]NMS, added after 30 min preincubation with the radioligand, or added at the same time before a further equilibration time of 2 or 6 h at 37 °C was employed. All other details are as described above.

1.8. PI accumulation assays

M_1 CHO cells were loaded overnight with [^{3}H]*myo*-inositol (1 μCi/ml) at 37 °C in a humidified incubator containing 5% CO_2/95% O_2. On the day of the experiment, cells were harvested and centrifuged (300 × *g*, 3 min), and the final pellet was re-suspended in 5 ml of HEPES buffer and used for cell counting. The cell suspension was then diluted in HEPES buffer containing 10 mM LiCl, distributed into assay tubes (∼ 500 000 cells/tube), and allowed to incubate for 15 min at 37 °C. After this pre-incubation period, drugs or appropriate vehicle controls (see below) were added to the remaining assay tubes and the reaction was allowed to proceed for a further 30 min (or in some cases 45 or 180 min; see Section 2) before being terminated by stop solution (methanol:chloroform, 2:1). Assay tubes were centrifuged at 450 × *g* for 5 min at room temperature, and total inositol phosphates were separated by ion exchange chromatography on Dowex AG1-X8 resin. The amount of radioactivity (dpm) in each sample was measured using a liquid scintillation counter and

values were corrected for recovery determined for each sample.

In initial experiments, concentration–response curves to ACh, butyryl choline (BCh), choline, tetramethylammonium (TMA) or anandamide were constructed. Agonist concentration–response curves were also reproduced in the presence of anandamide (10 or 100 μM), which was pre-incubated for 15 min before agonist addition. Different dilutions of ethanol were also used in place of anandamide concentrations to determine any vehicle effects.

In a separate series of experiments, M_1 CHO cells were treated with the alkylating agent, phenoxybenzamine (PBZ; 5 μM, 10 min) followed by extensive washout. This was performed in order to reduce the number of accessible binding sites for ACh prior to the establishment of agonist concentration–response curves. A range of ACh concentrations in the absence or presence of 10 μM anandamide were then tested as before.

1.9. Data analysis

Data sets of total and non-specific binding, derived from each complete saturation binding assay, were analyzed simultaneously via non-linear regression using Prism 4.0 (GraphPad Software, San Diego, CA). Analysis was performed according to a hyperbolic, one-site mass action binding model to derive individual estimates of total receptor density (B_{max}) and radioligand–receptor equilibrium dissociation constant (K_D) as shown in the following equation:

$$\text{total binding} = \frac{B_{max}\,x}{x + K_D} + \text{NS}x \quad (1)$$

where NS denotes non-specific binding and x denotes the concentration of the radioligand.

Radioligand inhibition binding isotherms were analyzed according to the following logistic function:

$$Y = \frac{(\text{top} - \text{bottom})x^{n_H}}{x^{n_H} + \text{IC}_{50}^{n_H}} \quad (2)$$

where Y denotes the percent specific binding, top and bottom denote the maximal and minimal asymptotes, respectively, x denotes the inhibitor concentration, IC_{50} denotes the inhibitor potency (midpoint location) parameter and n_H denotes the Hill slope factor. Where appropriate, and assuming simple competition, IC_{50} values were converted to K_i values (inhibitor equilibrium dissociation constant) using the Cheng and Prusoff (1973) equation.

Radioligand dissociation kinetic rates were evaluated by non-linear regression according to the following equation for mono-exponential decay using Prism 4.0:

$$Y = (a - b)\,e^{-k_{off}\cdot x} + b \quad (3)$$

where a represents the vertical span of the data, b is the plateau value, x is the time (min), and k_{off} is the dissociation rate constant (min^{-1}).

In functional assays, agonist concentration–response curves were fitted to the following four-parameter Hill equation using Prism 4.0:

$$\text{response} = \frac{(\text{top} - \text{bottom})}{1 + (10^{\log \text{EC}_{50}}/x)^{n_H}} \quad (4)$$

where top represents the maximal asymptote of the concentration–response curves, bottom represents the lowest asymptote of the concentration-response curves, log EC_{50} represents the logarithm of the agonist EC_{50}, x represents the concentration of the agonist, and n_H represents the Hill slope.

In all cases, potency and affinity values were estimated as logarithms [24]. Data shown are the mean ± S.E.M. Comparisons between mean values were performed by unpaired t tests whereas comparisons between models were performed by F-test using Prism. Unless otherwise stated, values of $p < 0.05$ were taken as statistically significant.

2. Results

2.1. Inhibition binding assays in CHO membranes

To examine the effects of anandamide on the binding of [^{3}H]NMS to M_1 CHO membranes, inhibition binding experiments were performed. Incubation of [^{3}H]NMS and anandamide for 1 h revealed that the endocannabinoid was able to completely inhibit radioligand binding at the M_1 mAChR, yielding a log IC_{50} of -5.55 ± 0.04 and n_H of 2.23 ± 0.42 ($n = 5$; Fig. 2A). The steep Hill slope for anandamide was significantly different from unity ($p < 0.05$) and was not due to an equilibration artifact, since extending the equilibration time to 4 h had no significant effect on the shape or the log IC_{50} value (-5.55 ± 0.04; $n = 8$) of the inhibition curve as compared to that derived from 1-h-equilibration studies (Fig. 2A).

2.2. Saturation binding assays in CHO membranes

[^{3}H]NMS saturation binding assays performed in M_1 CHO cell membranes revealed a trend for anandamide to reduce radioligand maximal binding capacity in a concentration dependent manner. Non-linear regression analysis of the data, followed by F-test, revealed that the simplest model accommodating all observations was a reduction in B_{max} with no change in radioligand affinity (log K_D of -9.63 ± 0.08; $n = 9$) with increasing presence of anandamide ($p > 0.05$).

2.3. Dissociation kinetic assays in CHO membranes

The inhibition and saturation binding assays indicated that anandamide interacts in a non-competitive manner

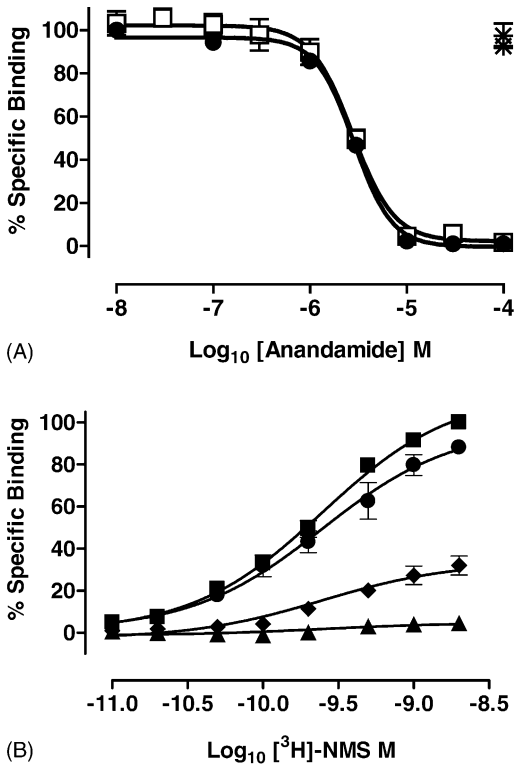

Fig. 2. Inhibition binding of anandamide or ethanol vehicle equivalents (✳) against 0.2 nM [^{3}H]NMS at the M_1 mAChR expressed in CHO cell membranes (Panel A). Incubation was for 1 (●) or 4 h (□) at 37 °C in HEPES buffer, pH 7.4 and non-specific binding was defined by 10 μM atropine. Data points represent the mean ± S.E.M. of 5–8 experiments conducted in duplicate. Saturation binding of [^{3}H]NMS in the absence (■) or presence of 1 (●), 5 (◆) or 10 μM (▲) anandamide in CHO membranes expressing the M_1 mAChR (Panel B). Incubation was for 1 h at 37 °C in HEPES buffer, pH 7.4. Non-specific binding was defined by 10 μM atropine. Data points represent the mean ± S.E.M. of 3–11 experiments conducted in duplicate. Where error bars are not shown they lie within the dimensions of the symbol.

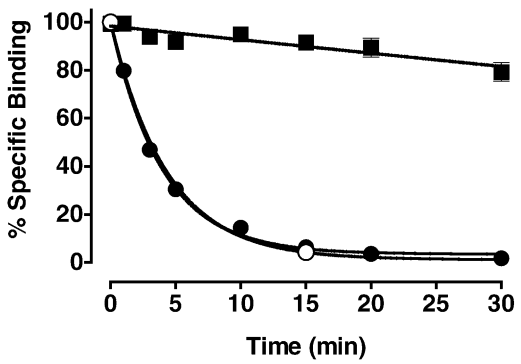

Fig. 3. Effect of anandamide on the dissociation rate of [^{3}H]NMS in CHO membranes expressing the M_1 mAChR. Membranes were incubated with 0.5 nM [^{3}H]NMS at 37 °C for 1 h in HEPES buffer, pH 7.4, before dissociation was revealed by addition of 1 μM atropine alone (●) or in combination with 10 μM anandamide (○), or by addition of 10 μM anandamide alone (■). Normalized curves represent the best fit via non-linear regression analysis (see Section 1.9). Data points represent the mean ± S.E.M. of three experiments conducted in duplicate. Where error bars are not shown they lie within the dimensions of the symbol.

with the M_1 mAChR. Many compounds that allosterically perturb mAChRs do so by altering the dissociation rate of orthosteric compounds, such as [^{3}H]NMS, at the receptor [25]. To determine whether anandamide possessed this property, [^{3}H]NMS dissociation kinetic assays were performed. Complete dissociation of [^{3}H]NMS, measured by isotopic dilution using excess atropine, was observed within 30 min at M_1 CHO membranes and yielded a k_{off} value of 0.25 ± 0.01 min^{-1} (n = 3). Repeating this experiment in the presence of anandamide had no effect on the dissociation rate of the radioligand (Fig. 3). Interestingly, when anandamide was added alone (i.e., in the absence of excess atropine) the dissociation of [^{3}H]NMS was only minimally visualized (k_{off} of 0.001 ± 0.037 min^{-1}; n = 3), indicating that anandamide had minimal influence on the rate of dissociation of [^{3}H]NMS that had been pre-equilibrated with the M_1 mAChR.

2.4. Anandamide washout and order-of-addition experiments

As described above, saturation binding experiments suggested that anandamide caused a reduction in [^{3}H]NMS maximal binding. To examine whether this inhibitory effect of the endocannabinoid on maximal binding capacity was due to an irreversible binding mechanism at the M_1 mAChR in CHO cells, washout experiments were performed. When anandamide was exposed to intact cells for 1 h followed by extensive washout, no effect on maximal [^{3}H]NMS binding was observed relative to vehicle-pretreated controls after either 10 μM (110 ± 8% relative to vehicle; n = 3) or 100 μM (93 ± 16% relative to vehicle; n = 4) anandamide pretreatment. This indicated a reversible mechanism of action for anandamide at the M_1 mAChR even at the high concentrations used.

To determine whether anandamide exhibited a persistent mode of binding that prevented [^{3}H]NMS binding to the M_1 mAChR, the order in which the agents were added was varied. These order-of-addition experiments revealed that incubation of anandamide (10 or 100 μM) before, after or at the same time as [^{3}H]NMS addition still resulted in significant inhibition of radioligand binding to M_1 CHO cells (Fig. 4). However, [^{3}H]NMS binding was least inhibited by either 10 or 100 μM anandamide when the radioligand was pre-incubated with the receptor for 30 min prior to addition of the endocannabinoid (Fig. 4). It is possible that this ''order of addition''-dependent inhibitory potency of anandamide reflected a lack of adequate total ligand–receptor equilibration time. However, when these experiments were repeated with a longer incubation time (6 h, using 10 μM anandamide), similar results were obtained (data not shown). In agreement with the dissociation kinetic assays, therefore, the inhibitory effect of anandamide is not as pronounced when the receptor is already occupied by radioligand.

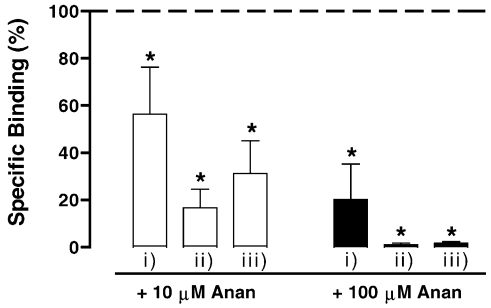

Fig. 4. Effect of changing ligand order of addition on the inhibition of 2 nM [^{3}H]NMS binding by 10 or 100 μM anandamide (Anan) at the M_1 mAChR expressed in intact CHO cells. Experiments were performed at 37 °C in HEPES buffer, pH 7.4, with specific binding of the radioligand alone (dashed line representing 100% bound). (i) [^{3}H]NMS was pre-incubated for 30 min before anandamide addition; (ii) anandamide was pre-incubated for 30 min prior to [^{3}H]NMS addition, or (iii) [^{3}H]NMS and anandamide were added simultaneously, before a further 90 min equilibration was employed. Data points represent the mean ± S.E.M. of 3–4 experiments conducted in quintuplicate. $^*p < 0.05$. Where error bars are not shown they lie within the dimensions of the symbol.

2.5. Ligand combination binding assays in CHO membranes

In order to gain further insight into potential site(s) on the M_1 mAChR with which anandamide may be interacting, [^{3}H]NMS inhibition binding assays were performed whereby anandamide was tested in the absence or presence of orthosteric agonists (ACh, Oxo-M, xanomeline), orthosteric antagonists (NMS, QNB) or prototypical allosteric modulators (gallamine, alcuronium). Fig. 5 illustrates a representative example of these experiments for an agonist, an antagonist and an allosteric modulator. Although the absolute specific binding of radioligand was consistently reduced in the presence of 3 μM anandamide, the endocannabinoid had no significant effect on the inhibitory potency of any of the mAChR ligands tested (Table 1), suggesting that anandamide did not share a common site of action with any of these classes of compounds.

2.6. Effect of increasing membrane content on the inhibitory properties of anandamide

Given anandamide's lipophilic nature, and the fact that the combination binding experiments described above indicated that anandamide did not appear to interact via classic extracellular binding domains on the M_1 mAChR, additional experiments were performed to determine the extent to which incorporation into the cell membrane is important for the actions of anandamide. In these experiments, anandamide was pre-incubated with NT CHO cell membranes prior to addition of M_1 CHO membranes. As shown in Fig. 6A, the binding isotherm for anandamide was shifted to the right with increasing concentrations of pre-incubated NT CHO membranes. The most prominent

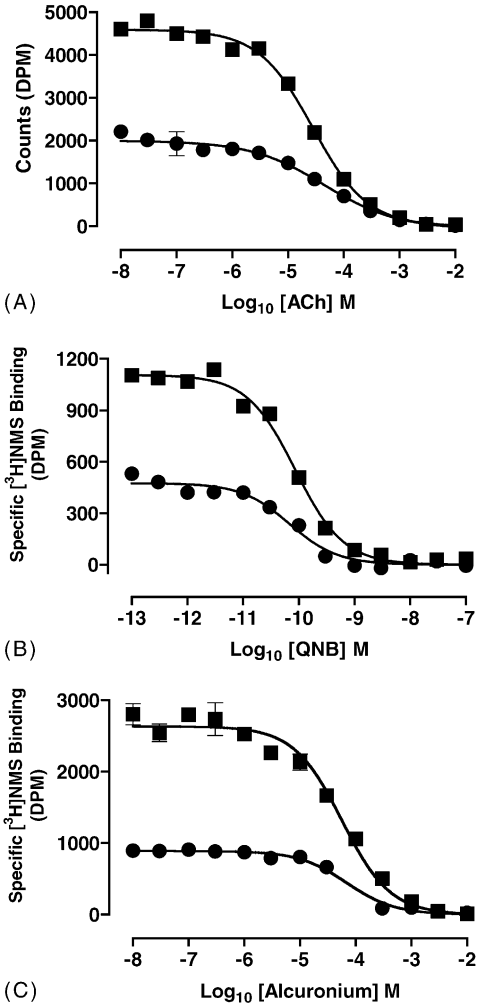

Fig. 5. Inhibition binding of the agonist, ACh (A), antagonist, QNB (B), or allosteric modulator, alcuronium (C) against 0.2 nM [^{3}H]NMS in the absence (■) or presence (●) of 3 μM anandamide at the M_1 mAChR expressed in CHO cell membranes. Incubation was for 1 h at 37 °C in HEPES buffer, pH 7.4 and non-specific binding was defined by 10 μM atropine. All figures represent raw data in dpm from individual experiments. Where error bars are not shown they lie within the dimensions of the symbol.

shift in the inhibitory potency of anandamide against [^{3}H]NMS at the M_1 mAChR was after pre-incubation with 100 μg/ml of NT CHO membranes, as indicated by a log IC_{50} value of −4.21 ± 0.04 (n = 3), as compared to

Table 1
Binding potency values for competition between various mAChR ligands against 0.2 nM [^{3}H]NMS at M_1 mAChRs expressed in CHO cell membranes

Ligand	log IC_{50}[a]		n[b]
	Vehicle	+Anandamide (3 μM)	
ACh	−4.67 ± 0.17	−4.31 ± 0.12	5
Oxo-M	−4.74 ± 0.20	−4.66 ± 0.03	3
Xanomeline	−6.31 ± 0.18	−6.04 ± 0.09	3
NMS	−9.30 ± 0.08	−9.23 ± 0.04	3
QNB	−10.20 ± 0.07	−10.12 ± 0.08	5
Gallamine	−6.14 ± 0.03	−6.07 ± 0.03	3
Alcuronium	−4.30 ± 0.03	−4.23 ± 0.07	3

[a] Negative logarithm of the IC_{50}.
[b] Number of experiments.

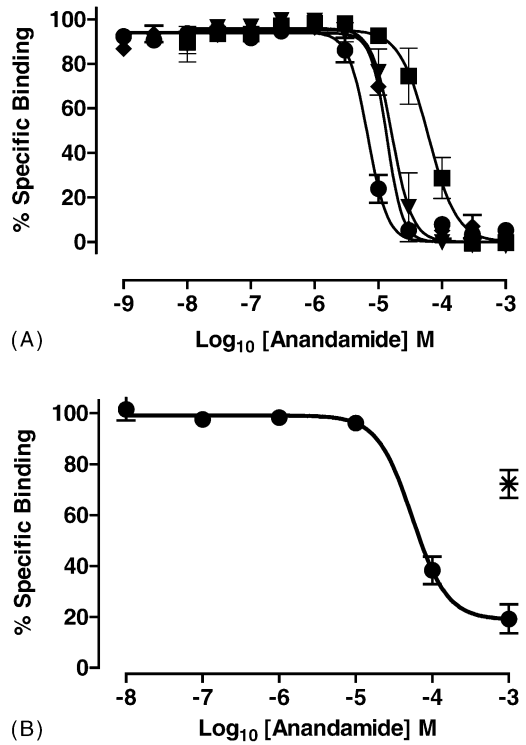

Fig. 6. (A) Inhibition binding of anandamide against 0.2 nM [^{3}H]NMS in the absence (●) or presence of 10 (◆), 25 (▼) or 100 μg/ml (■) NT CHO membranes in combination with 10 μg/ml of CHO membranes expressing the M_1 mAChR. Incubation with non-transfected CHO membranes was for 30 min prior to M_1 mAChR addition and the reaction was allowed to proceed for a further 1 h at 37 °C in HEPES buffer, pH 7.4. Data points represent the mean ± S.E.M. of 3–8 experiments conducted in duplicate. Where error bars are not shown they lie within the dimensions of the symbol. (B) Inhibition binding of anandamide (●), or ethanol vehicle equivalent (✳) against 0.2 nM [^{3}H]NMS at the M_1 mAChR expressed in intact CHO cells. Data points represent the mean ± S.E.M. of four experiments conducted in duplicate. Where error bars are not shown they lie within the dimensions of the symbol.

a log IC_{50} of −5.16 ± 0.03 (n = 8) for the NT CHO membrane-free inhibition curve of anandamide. This represents a significant ($p < 0.05$) 10-fold shift in potency for the endocannabinoid at the M_1 mAChR in the presence of NT CHO membranes.

One possible parsimonious explanation for these findings is that anandamide can, in fact, interact competitively with the M_1 mAChR, and that its apparent non-competitive effects simply reflect its ability to be adsorbed, or otherwise deposited, into the membrane via a saturable removal process. The predictions of such a model were investigated using simulations, as outlined in the Appendix A. The salient features of the model with respect to our experimental observations are that an increase in the capacity of the removal process, as would be observed, for example, by increases in the level of NT CHO membranes, would result in a commensurate reduction in inhibitory potency (as was observed experimentally) and a significant increase in the Hill slope (see Appendix A). In our experiments, the Hill slopes ranged from 2.4 ± 0.7 in the absence of membrane to 1.8 ± 0.3 in the presence of the highest concentration of membrane. This latter finding argues against a simple model of competition coupled with a saturable removal mechanism as the minimal mechanism underlying our observations.

In order to further investigate the role of the membrane environment on anandamide potency, further experiments were undertaken in the absence or presence of 100 μM NT CHO membranes at 4 °C. In the absence of NT CHO membranes, the log IC_{50} value of anandamide was reduced to 4.90 ± 0.03 (n = 3; 3 h incubation), and in the presence of NT CHO membranes, the value was 4.60 ± 0.04 (n = 4). These results indicate that the reduction of membrane fluidity at low temperatures affects the inhibitory potency of anandamide.

2.7. Inhibition binding assays at M_1 mAChRs in intact CHO cells

In a separate series of experiments, the potency of anandamide was examined against [^{3}H]NMS in intact CHO cells expressing M_1 mAChRs. As with the membrane-based binding assays, steep binding isotherms for anandamide were also observed in intact CHO cells (Fig. 6B), with a Hill slope of 1.83 ± 0.15 (n = 4). The most significant effect, however ($p < 0.05$), was an approx. Ten-fold loss of potency for anandamide in intact cells as compared to membranes, with a log IC_{50} of −4.24 ± 0.11 (n = 4).

2.8. PI accumulation assays

To determine whether the inhibitory effects of anandamide extended to cellular function mediated by M_1 mAChRs, second messenger experiments were conducted in M_1 CHO cells measuring PI accumulation under similar assay conditions to those used in radioligand binding experiments. As shown in Fig. 7A, 45 min incubation of the cells with ACh led to a concentration-dependent accumulation of total radiolabelled inositol phosphates. On its own, anandamide had no effect (not shown). Interestingly, the addition of 10 μM anandamide, which was sufficient to fully abolish radioligand binding in CHO M_1 membranes, failed to inhibit the PI response to ACh. However, increasing the concentration of anandamide 10-fold resulted in an approximate 35% reduction in the maximal response to ACh (Table 2). Similar results were obtained when ACh incubation time was increased to 180 min (Fig. 7B; Table 2).

When compared to the amount of anandamide required to abolish [^{3}H]NMS binding in radioligand binding assays, the reduction in maximal ACh responses required a much higher concentration of endocannabinoid. This may reflect a high level of receptor reserve for ACh and/or a lower potency of anandamide to influence ligand binding in intact cells. To reduce the amount of receptor reserve in the system, and thus limit the number of accessible binding sites for ACh, alkylation experiments using PBZ (5–

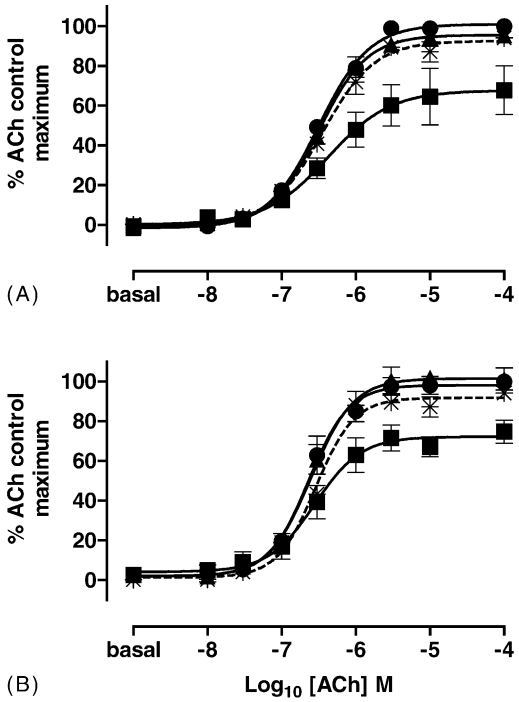

Fig. 7. Concentration–response curves for ACh-mediated PI accumulation in the absence (●) and presence of 10 μM (▲) or 100 μM (■) anandamide or ethanol vehicle (✳) in M_1 CHO cells. Cells were equilibrated with anandamide or vehicle control for 15 min at 37 °C before the addition of ACh for an additional 30 min (Panel A) or 165 min (Panel B) in HEPES buffer. Parameter values from logistic curve-fitting via nonlinear regression are indicated in Table 2. Data points are mean ± S.E.M. of 3–9 experiments conducted in triplicate. Where error bars are not shown they lie within the dimensions of the symbol.

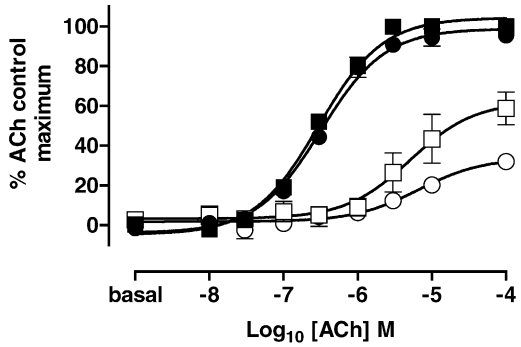

Fig. 8. Effects of M_1 mAChR alkylation on ACh-mediated PI accumulation. M_1 CHO cells without (closed symbols), or with PBZ (5 μM for 10 min followed by washout; open symbols) were incubated with increasing concentrations of ACh in the absence (squares) or presence (circles) of 10 μM anandamide. Data points are mean ± S.E.M. of 4–12 experiments conducted in triplicate. Where error bars are not shown they lie within the dimensions of the symbol.

10 μM) were performed. Under these conditions, anandamide (10 μM) was indeed able to produce a significant reduction in the E_{max} (25 ± 10%; $n = 4$) for ACh as compared to its effects at untreated M_1 CHO cells ($p < 0.05$; Fig. 8).

From the membrane-based binding experiments, it also appeared that the effects of anandamide were more prominent with NMS than with ACh. This may simply reflect assay conditions, as the inhibitory potency of anandamide against NMS was significantly reduced in intact cells (see above), and all functional assays were conducted in intact cells. However, another possibility may also be related to the potential for differential steric hindrance effects related to the size of the agents (mAChR antagonists are generally larger molecules than agonists). Therefore, to determine whether the effects of anandamide on PI hydrolysis were governed by the size of the molecule binding to the M_1 mAChR, a separate series of experiments were performed using several mAChR agonists that varied in size and structure (Fig. 1). All of the agonists tested were able to stimulate M_1 mAChR-mediated PI hydrolysis with the following rank order of maximum agonist effect, ACh ≥ TMA > BCh > choline (Fig. 9). Thus, the latter two agents, in particular, were partial agonists relative to ACh, and would not be expected to possess receptor reserve for their effects on PI hydrolysis.

As described previously, when the highest efficacy agonist, ACh, was used to mediate PI production, 10 μM anandamide had no effect on the agonist concentration–response curve unlike the much higher concentration of the endocannabinoid, which reduced the E_{max} significantly (Fig. 7; Table 3). When TMA was used, a similar trend was noted, with no effect observed with 10 μM anandamide but a significant reduction in the maximal agonist response being achieved with 100 μM anandamide (Fig. 10A; Table 3). However, when the lower efficacy agonist BCh was used, 10 μM anandamide sig-

Table 2
Concentration–response curve parameters for ACh-mediated PI hydrolysis in the absence or presence of anandamide at M_1 mAChRs expressed in CHO cells

Parameters	45 min equilibration time			180 min equilibration time		
	Vehicle	+10 μM anandamide	+100 μM anandamide	Vehicle	+10 μM anandamide	+100 μM anandamide
E_{max}[a]	100	96 ± 1*	66 ± 14*	100	103 ± 5	74 ± 6*
log EC_{50}[b]	−6.53 ± 0.04	−6.49 ± 0.03	−6.29 ± 0.12*	−6.64 ± 0.08	−6.60 ± 0.07	−6.58 ± 0.15
n_H[c]	1.36 ± 0.03	1.24 ± 0.09	1.02 ± 0.20*	1.56 ± 0.11**	1.45 ± 0.19	1.32 ± 0.40

Parameters represent the mean ± S.E.M. of 4–13 experiments.
[a] Maximum effect, expressed as percentage of the vehicle-treated ACh maximum response.
[b] Logarithm of the EC_{50}.
[c] Hill slope factor.
* Student's *t*-test found a significant ($p < 0.05$) difference between control and anandamide-treated groups.
** Student's *t*-test found a significant ($p < 0.05$) difference between 45 and 180 min equilibration time groups.

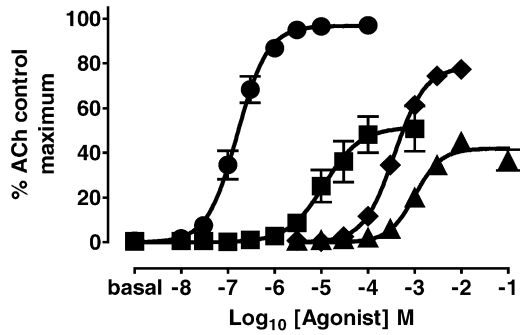

Fig. 9. Concentration–response curves for mAChR agonist-mediated PI accumulation. M_1 CHO cells were incubated with increasing concentrations of ACh (●), BCh (■), TMA (◆), or choline (▲). Parameter values from logistic curve-fitting via nonlinear regression are indicated in Table 3. Data points are mean ± S.E.M. of 4–10 experiments conducted in triplicate. Where error bars are not shown they lie within the dimensions of the symbol.

nificantly reduced the E_{max} for the agonist ($p < 0.05$), and 100 μM anandamide almost completely inhibited BCh-mediated PI responses (Fig. 10B; Table 3). A similar effect was noted with another low efficacy agonist, choline, with a significant reduction in E_{max} for choline in the presence of 100 μM anandamide ($p < 0.05$; Fig. 10C; Table 3).

These results suggest that the size of the agonists (rank order of size BCh > ACh > choline > TMA; Fig. 1) did not determine the magnitude of effect that anandamide exerted at the M_1 mAChR. Instead of anandamide having a steric hindrance effect with these agonists, it would appear that its effects at the M_1 mAChR are agonist-dependent, with lower efficacy agonists being more influenced than higher ones.

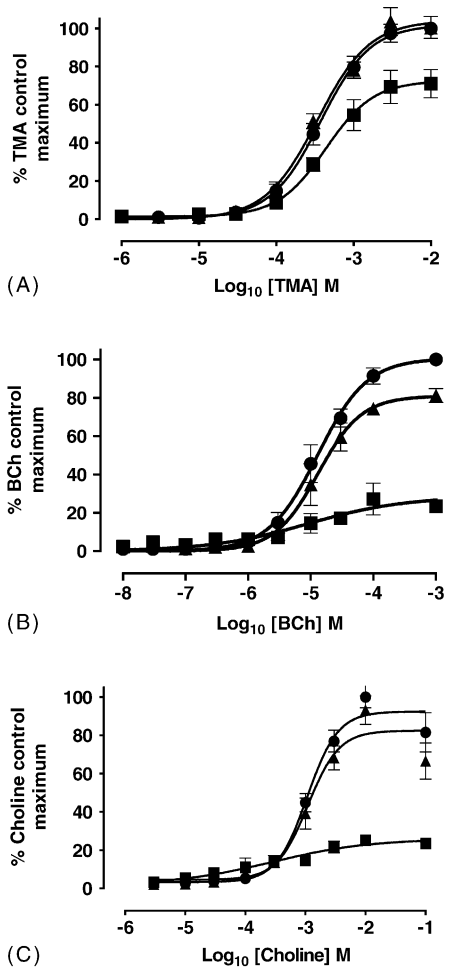

Fig. 10. Concentration–response curves for TMA: (Panel A), BCh: (Panel B) and choline: (Panel C) mediated PI accumulation in the absence (●) and presence of 10 (▲) or 100 μM (■) anandamide in M_1 CHO cells. Parameter values from logistic curve-fitting via nonlinear regression are indicated in Table 3. Data points are mean ± S.E.M. of 4–10 experiments conducted in triplicate. Where error bars are not shown they lie within the dimensions of the symbol.

3. Discussion

ACh and the endogenous cannabinoid, anandamide, exert profound, albeit opposing, regulatory effects on learning and memory. Although ACh mediates most of its effects through M_1 mAChRs and anandamide through interaction with CB_1 cannabinoid receptors, studies have recently demonstrated a direct effect of anandamide on antagonist binding to the mAChRs [21,22]. The present study confirms and extends these previous findings, and suggests that anandamide may interact with the M_1 mAChR through a mechanism not shared by classical or allosteric drugs. The interaction of anandamide at this receptor is non-competitive in nature and likely involves perturbation of the membrane.

The direct effects of anandamide at the M_1 mAChR expressed in CHO cell membranes resulted in complete

Table 3
Concentration–response curve parameters for M_1 mAChR-mediated PI hydrolysis using a range of mAChR agonists in the absence or presence of anandamide

Agonist	Vehicle			+10 μM anandamide			+100 μM anandamide		
	E_{max} [a]	log EC_{50} [b]	n_H [c]	E_{max} [a]	log EC_{50} [b]	n_H [c]	E_{max} [a]	log EC_{50} [b]	n_H [c]
ACh	100	−6.53 ± 0.04	1.36 ± 0.03	96 ± 1*	−6.49 ± 0.03	1.24 ± 0.09	66 ± 14*	−6.32 ± 0.21	1.02 ± 0.20*
TMA	75 ± 3	−3.49 ± 0.05	1.57 ± 0.11	74 ± 5	−3.55 ± 0.05	1.63 ± 0.18	49 ± 5*	−3.44 ± 0.03	1.69 ± 0.30
BCh	52 ± 8	−4.92 ± 0.12	1.30 ± 0.06	41 ± 9	−4.88 ± 0.15	1.55 ± 0.11	17 ± 6*	−4.85 ± 0.16	0.91 ± 0.21
Choline	44 ± 3	−2.95 ± 0.04	1.54 ± 0.12	37 ± 4	−2.99 ± 0.05	1.81 ± 0.28	14 ± 3*	−3.47 ± 0.63	0.34 ± 0.05*

Parameters represent the mean ± S.E.M. of 4–13 experiments. Letters (shown in superscripts [a,b,c]), as described before in Table 2.
* Student's *t*-test found a significant ($p < 0.05$) difference between vehicle- and anandamide-treated groups.

abolition of [^{3}H]NMS binding that was characterized by very steep inhibition curves for the endocannabinoid (Hill slopes greater that unity). These steep binding isotherms were not due to inadequate equilibration time for the low-anandamide concentrations and are not in accord with the predictions of simple mass action kinetics, indicating a non-competitive mode of interaction. [^{3}H]NMS saturation binding assays further confirmed the non-competitive behavior of anandamide, and indicated that the effect of the endocannabinoid was to reduce the maximum capacity of radioligand binding sites (B_{max}) with no significant effect on K_D. This finding is at odds with our previous study, which found that anandamide was able to reduce both B_{max} and K_D of [^{3}H]QNB in saturation binding assays, although the effect on [^{3}H]QNB affinity at the M_1 mAChR was modest [22]. Based on a number of findings from our current study, however, we believe that our earlier observation of an apparent effect of anandamide on [^{3}H]QNB affinity is possibly an artifact related to the preference of the nonlinear regression algorithm to apportion a significant, albeit small, difference in [^{3}H]QNB values. Specifically, in our current work [^{3}H]NMS competition against QNB in the absence or presence of anandamide (Fig. 5) revealed no effect of the endocannabinoid on QNB potency (Table 1); these competition-style binding assays have an advantage over saturation assays in that a much wider range of QNB concentrations can be utilized in the competition assay relative to the saturation assay. Second, when tested against other orthosteric ligands in both competition (Table 1) and functional assays, there was no indication of anandamide affecting ligand potency; the functional assays were characterized only by a non-competitive reduction in E_{max} by anandamide (Table 3), which is consistent with an effect of the endocannabinoid on maximal M_1 mAChR binding sites but not affinity.

To more readily ascertain whether the non-competitive action of anandamide in reducing [^{3}H]NMS binding was due to an allosteric influence on the rate at which NMS dissociates from the M_1 mAChR in CHO membranes, kinetic assays were performed. The rate of dissociation of [^{3}H]NMS from the M_1 mAChR in the presence of atropine, was not altered by anandamide suggesting an action unlike those of prototypical allosteric modulators; a hallmark of these latter types of modulators is their ability to change orthosteric ligand dissociation by altering the conformation of the receptor. This change in receptor conformation would be expected to result in an alteration of orthosteric ligand association and/or dissociation characteristics [25]. It is this alteration in [^{3}H]NMS kinetics that underlies the effects of many allosteric modulators on NMS affinity at equilibrium, and this is not seen with anandamide in the current study.

A reduction in radioligand B_{max}, seen with anandamide in saturation binding assays, is a property that has been noted for ligands that bind to receptors in an irreversible manner. However, this was not the case for anandamide when [^{3}H]NMS maximal binding was unaffected in CHO cells that were pretreated with moderate to high concentrations of anandamide followed by extensive washout.

Although anandamide's mechanism of action was reversible, the magnitude of its effect clearly varied with the order of exposure of the endocannabinoid to the receptor. To determine whether this influenced the inhibitory properties of the endocannabinoid, the order of addition of anandamide and [^{3}H]NMS was varied, with simultaneous administration of the two ligands reflecting standard experimental conditions. The least inhibitory effect on [^{3}H]NMS binding occurred when the radioligand was equilibrated for half an hour before anandamide was administered, and did not change any further over a 6 h time period. This indicated that the effect of anandamide is least pronounced when the receptor is already occupied by an mAChR ligand, suggesting that the order of addition of the endocannabinoid may be more crucial than the time of equilibration with the receptor. These results were in good agreement with those obtained from dissociation kinetic assays, where anandamide was very weak in preventing re-association of the radioligand that had been pre-equilibrated with the M_1 mAChR.

Although anandamide influences NMS binding properties, its site of action appears to be distinct from that of orthosteric ligands, and is reflected in its non-competitive behavior at the M_1 mAChR. This was further confirmed using a range of mAChR pharmacological tools (agonists, antagonists and allosteric modulators) in combination with [^{3}H]NMS and anandamide. It was found that the action of the endocannabinoid was not via the classic agonist/antagonist orthosteric site or the well-defined allosteric binding site on the M_1 mAChR recognized by gallamine and alcuronium. However, another study has shown that anandamide was able to influence the agonist binding properties of [^{3}H]Oxo-M [21]. In that study, inhibition of [^{3}H]Oxo-M was produced using a concentration of anandamide 50-fold higher than those used in the binding studies of the current investigation. This suggests that to obtain an effect of anandamide on agonist binding in the present study, higher concentrations of the endocannabinoid would need to be employed. Ion levels have also been shown to play a role in determining the effectiveness of G protein coupling to the receptor [26]. However, when the buffer was varied in our binding studies, anandamide still had no effect on ACh binding at the M_1 mAChR and its action appeared to be insensitive to the ion composition of the buffer (data not shown).

It was further hypothesized that anandamide may be preferentially accessing the M_1 mAChR by the membrane. Equilibration of anandamide with [^{3}H]NMS and non-transfected CHO cell membranes, before the introduction of M_1 CHO membranes, resulted in a marked reduction of anandamide's potency to inhibit radioligand binding at the

receptor. Simulations based on a competitive model of ligand–receptor interaction coupled with a saturable removal process for anandamide (see Appendix A), could not account for our experimental observations, suggesting that the interaction between the endocannabinoid and the M_1 mAChR is truly non-competitive. Our results could thus be reconciled with a mechanism of action for cannabinoids that is via membrane perturbation, affecting the functioning of membrane-associated proteins such as GPCRs [27]. Indeed, it has also been reported that the action of anandamide is not only limited to interaction with receptors but may also involve alterations in membrane or lipid bilayer organization. A study by Bloom et al. [28] suggested that membrane perturbation (measured as an increase or decrease in lipid order of rat brain synaptic plasma membranes) caused by anandamide and a number of other nonclassical and endogenous cannabinoids, may be a necessary property for the pharmacological activity of this class of drugs. However, this is unlikely to be the case for mAChRs, as we have previously found that the inhibitory effects of anandamide on mAChRs are likely due to its eicosanoid structure, rather than its canabinomimetic properties [22]. Nonetheless, experiments conducted at 4 °C, which results in reduced membrane fluidity, revealed a reduction in both anandamide's inhibitory potency against [^{3}H]NMS and the ability of non-transfected CHO membranes to further adsorb anandamide, lending additional support to a role of membrane deposition in anandamide's ability to interact with the M_1 mAChR.

Results obtained from the radioligand binding assays specifically examined the effects of anandamide on ligand binding, and showed that anandamide had a greater effect on [^{3}H]NMS binding in membranes than in intact CHO cells (10-fold loss in potency) and no effect on agonist binding to the M_1 mAChR. These results suggested that anandamide's inhibitory effect was via disruption of the membrane milieu and more pronounced in broken cell preparations. To address this, intact cell functional assays were employed. Specifically, the functional consequences of the interaction between anandamide and the M_1 mAChR were investigated using PI accumulation assays in intact CHO cells. Anandamide has no agonistic properties in this system, but was able to significantly reduce the maximal response for the agonist, ACh, with only a minimal effect on agonist potency. However, the concentration of anandamide (100 μM) used to produce this effect was far in excess of those used in radioligand binding assays. It is possible that the anandamide binding site is found at a more intracellular level, or at the receptor–membrane interface, which would explain its enhanced potency in membrane-based binding assays.

Reducing the amount of M_1 mAChR reserve for ACh enhanced the inhibitory effect of a lower concentration of anandamide (10 μM), that would normally have no effect on E_{max} for the agonist. This suggested that anandamide may be more influential on the function of partial agonists rather than full agonists. It was also hypothesized that anandamide had a greater 'steric hindrance' effect with the antagonist, NMS, than with the agonist, ACh. To address both issues, further PI assays were conducted using a wide range of mAChR agonists (BCh, ACh, choline and TMA) that varied in size and efficacy. From these studies, the size of the agonist did not determine the degree of efficacy at the M_1 mAChR. ACh and TMA were found to be the most efficacious agonists, with BCh and choline displaying much lower efficacy at the M_1 mAChR. The most striking results with anandamide (100 μM) were obtained with the lower efficacy agonists, BCh and choline. Anandamide profoundly inhibited the maximal agonist responses for each agonist. This suggested that agonist sensitivity to inhibition by anandamide is related to ligand efficacy and not the size of the molecule.

At present, it is difficult to make unambiguous statements regarding the overall physiological significance of these findings. Although the effects of anandamide on M_1 mAChRs observed in our current study occur at concentrations that are significantly higher than those reported to be normally present in the brain [29], significant elevations of anandamide have been noted in certain pathological states [19–20]. Furthermore, accurate determinations of true anandamide concentrations at the level of the receptor–membrane compartment are difficult to obtain [30]. Further, insight into the role of mAChR–anandamide interactions may possibly be gleaned from studies utilizing FAAH knockout mice [31], but to our knowledge such investigations have yet to be undertaken.

In conclusion, there are several points that can be drawn from the current investigation about the interaction of anandamide with the M_1 mAChR: (1) the effect of anandamide is to reduce receptor accessibility for various ligands, (2) for antagonists, this is clearly evident in direct assays of [^{3}H]-antagonist binding whereas for agonists, this is most apparent when there is no receptor reserve, (3) anandamide is less potent in intact cells than membranes and (4) the mechanism of anandamide inhibition of M_1 mAChR action is most likely by perturbing the receptor via the membrane but is sensitive to the conformation of the receptor (occupied versus vacant). These findings suggest that the direct effects of anandamide on mAChR function are likely to be minimal under normal physiological conditions, but can become specifically relevant in schizophrenia or various ischemic states where elevated levels of anandamide have been noted.

Acknowledgments

The authors are grateful to Dr. Fred Mitchelson for helpful discussions. This work was funded by Project Grant No. 209083 of the National Health and Medical

Research Council (NHMRC) of Australia. Arthur Christopoulos is a senior research fellow of the NHMRC.

Appendix A

A model was constructed to simulate the effects of a saturable removal process from the receptor compartment on the concentration of an unlabelled ligand that would otherwise interact competitively with a radioligand. It was assumed that the concentration of unlabelled ligand X that is free in the receptor compartment, $[X_F]$, is equal to the difference between the total concentration of ligand that is added, $[X_T]$, and the concentration of ligand that is adsorbed, or otherwise removed, from the receptor compartment, $[X_{Ad}]$. In the specific case of anandamide, it is unlikely that this removal process is metabolic but more likely to reflect some form of membrane deposition; there are no known anandamide removal mechanisms in CHO cells [32], and our studies, which have utilized incubation periods ranging from approximately 2 to 6 h, found no evidence for any other degradative processes that would be expected to reduce anandamide potency in a time-dependent manner.

The model assumes that the removal process is reversible and saturable, such that the concentration of ligand bound at the site of adsorption/removal is given by:

$$[X_{Ad}] = \frac{([X_T] - [X_{Ad}])\text{Max}}{[X_T] - [X_{Ad}] + K_{Ad}} \quad (A.1)$$

where Max denotes the maximal capacity of the adsorption/removal process in terms of binding sites, and K_{Ad} denotes the equilibrium dissociation constant for the adsorption binding event. Because this is an implicit equation with respect to $[X_{Ad}]$, Eq. (A.1) can be rearranged as a standard quadratic of the form:

$$[X_{Ad}]^2 - (\text{Max} + [X_T] + K_{Ad})[X_{Ad}] + [X_T]\text{Max} = 0 \quad (A.2)$$

One solution for this quadratic equation is:

$$\frac{[X_T] + K_{Ad} + \text{Max} - \sqrt{([X_T] + K_{Ad} + \text{Max})^2 - 4[X_T]\text{Max}}}{2} \quad (A.3)$$

Since $[X_F] = [X_T] - [X_{Ad}]$, then

$$[X_F] = [X_T] - \frac{[X_T] + K_{Ad} + \text{Max} - \sqrt{([X_T] + K_{Ad} + \text{Max})^2 - 4[X_T]\text{Max}}}{2} \quad (A.4)$$

Eq. (A.4) was used to provide the values of ligand free in the receptor compartment ($[X_F]$) for simulating a simple bimolecular competitive interaction between the ligand and a radiolabelled competitor under various degrees of ligand adsorption (i.e., differing values of Max), as shown in Fig. 11.

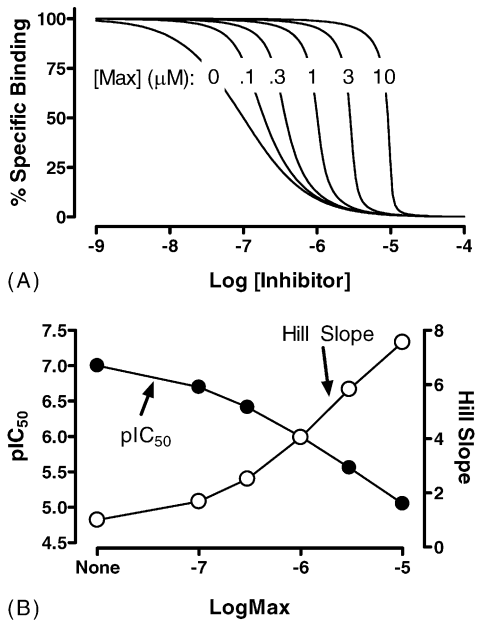

Fig. 11. Theoretical simulations, based on Eq. (A.4) of the Appendix A, depicting the effect of a saturable ligand removal process on the ability of an inhibitor to compete with a radioligand for specific receptor binding. (A) Inhibition binding assay. The following parameters were used: $\log K_D$ (radioligand) = −9.7; [radioligand] = 0.2 nM; $\log K_D$ (inhibitor) = −7.3; $\log K_{Ad}$ = −8; maximal binding capacity (Max) of sites of removal were varied as shown in the Panel. (B) Effects of increasing the maximal binding capacity (Max) of saturable removal sites for a competitive inhibitor on estimates of inhibitor potency (pIC_{50}) and Hill Slope. Parameter estimates were obtained by fitting the Hill equation (Eq. (4) in Section 1) to the data shown in Panel A.

References

[1] Hampson RE, Deadwyler SA. Role of cannabinoid receptors in memory storage. Neurobiol Dis 1998;5:474–82.
[2] Hampson RE, Deadwyler SA. Cannabinoids, hippocampal function and memory. Life Sci 1999;65:715–23.
[3] Jerusalinsky D, Kornisiuk E, Izquierdo I. Cholinergic neurotransmission and synaptic plasticity concerning memory processing. Neurochem Res 1997;22:507–15.
[4] Ladner CJ, Lee JM. Pharmacological drug treatment of Alzheimer disease: the cholinergic hypothesis revisited. J Neuropathol Exp Neurol 1998;57:719–31.
[5] Segal M, Auerbach JM. Muscarinic receptors involved in hippocampal plasticity. Life Sci 1997;60:1085–91.
[6] Caulfield MP. Muscarinic receptors-characterization, coupling and function. Pharmacol Ther 1993;58:319–79.
[7] Caulfield MP, Birdsall NJ. International Union of Pharmacology. XVII. Classification of muscarinic acetylcholine receptors. Pharmacol Rev 1998;50:279–90.
[8] Pertwee RG. Cannabinoid receptor ligands: clinical and neuropharmacological considerations, relevant to future drug discovery and development. Expert Opin Invest Drugs 2000;9:1553–71.
[9] Pertwee RG, Ross RA. Cannabinoid receptors and their ligands. Prostaglandins Leukot Essent Fatty Acids 2002;66:101–21.
[10] Friedman MA. Inhibition of arylhydrocarbon hydroxylase induction in BALB/C mouse liver by Δ9-tetrahydrocannabinol. Res Commun Chem Pathol Pharmacol 1976;15:541–52.

[11] Domino EF, Bartolini A. Effects of various psychotomimetic agents on the EEG and acetylcholine release from the cerebral cortex of brainstem transected cats. Neuropharmacology 1972;11:703–13.
[12] Braida D, Sala M. Cannabinoid-induced working memory impairment is reversed by a second generation cholinesterase inhibitor in rats. Neuroreport 2000;11:2025–9.
[13] Terranova JP, Storme JJ, Lafon N, Perio A, Rinaldi-Carmona M, Le Fur G, et al. Improvement of memory in rodents by the selective CB1 cannabinoid receptor antagonist, SR 141716. Psychopharmacology Berl 1996;126:165–72.
[14] Di Marzo V, Breivogel CS, Tao Q, Bridgen DT, Razdan RK, Zimmer AM, et al. Levels, metabolism, and pharmacological activity of anandamide in CB1 cannabinoid receptor knockout mice: evidence for non-CB1, non-CB2 receptor-mediated actions of anandamide in mouse brain. J Neurochem 2000;75:2434–44.
[15] Zygmunt PM, Petersson J, Andersson DA, Chuang H, Sorgard M, Di Marzo V, et al. Vanilloid receptors on sensory nerves mediate the vasodilator action of anandamide. Nature 1999;400:452–7.
[16] Di Marzo V, De Petrocellis L, Fezza F, Ligresti A, Bisogno T. Anandamide receptors. Prostaglandins Leukot Essent Fatty Acids 2002;66:377–91.
[17] Parolaro D, Massi P, Rubino T, Monti E. Endocannabinoids in the immune system and cancer. Prostaglandins Leukot Essent Fatty Acids 2002;66:319–32.
[18] Kimura T, Ohta T, Watanabe K, Yoshimura H, Yamamoto I. Anandamide, an endogenous cannabinoid receptor ligand, also interacts with 5-hydroxytryptamine (5-HT) receptor. Biol Pharm Bull 1998;21:224–6.
[19] Leweke FM, Giuffrida A, Wurster U, Emrich HM, Piomelli D. Elevated endogenous cannabinoids in schizophrenia. Neuroreport 1999;10:1665–9.
[20] Felder CC, Glass M. Cannabinoid receptors and their endogenous agonists. Annu Rev Pharmacol Toxicol 1998;38:179–200.
[21] Lagalwar S, Bordayo EZ, Hoffmann KL, Fawcett JR, Frey II WH. Anandamides inhibit binding to the muscarinic acetylcholine receptor. J Mol Neurosci 1999;13:55–61.
[22] Christopoulos A, Wilson K. Interaction of anandamide with the M1 and M4 muscarinic acetylcholine receptors. Brain Res 2001;915:70–8.
[23] Bradford MM. A rapid and sensitive method for the quantitation of microgram quantities of protein utilizing the principle of protein–dye binding. Anal Biochem 1976;72:248–54.
[24] Christopoulos A. Assessing the distribution of parameters in models of ligand–receptor interaction: to log or not to log. Trends Pharmacol Sci 1998;19:351–7.
[25] Christopoulos A, Kenakin T. G protein-coupled receptor allosterism and complexing. Pharmacol Rev 2002;54:323–74.
[26] Ladner CJ, Lee JM. Reduced high-affinity agonist binding at the M1 muscarinic receptor in Alzheimer's disease brain: differential sensitivity to agonists and divalent cations. Exp Neurol 1999;158:451–8.
[27] Martin BR. Cellular effects of cannabinoids. Pharmacol Rev 1986;38:45–74.
[28] Bloom AS, Edgemond WS, Moldvan JC. Nonclassical and endogenous cannabinoids: effects on the ordering of brain membranes. Neurochem Res 1997;22:563–8.
[29] Fride E, Di Marzo V. Endocannabinoids. Eur J Pharmacol 1998;359:1–18.
[30] Piomelli D, Beltramo M, Giuffrida A, Stella N. Endogenous cannabinoid signaling. Neurobiol Dis 1998;5:462–73.
[31] Cravatt BF, Demarest K, Patricelli MP, Bracey MH, Giang DK, Martin BR, et al. Supersensitivity to anandamide and enhanced endogenous cannabinoid signaling in mice lacking fatty acid amide hydrolase. Proc Natl Acad Sci USA 2001;98:9371–6.
[32] Gonsiorek W, Lunn C, Fan X, Narula S, Lundell D, Hipkin RW. Endocannabinoid 2-arachidonyl glycerol is a full agonist through human type 2 cannabinoid receptor: antagonism by anandamide. Mol Pharmacol 2000;57:1045–50.